ACS APPLIED NANO MATERIALS

www.acsanm.org Article

One-Step Conversion of Graphite to Crinkled Boron Nitride Nanofoams for Hydrophobic Liquid Absorption

Thang Pham,[▽] Scott Stonemeyer,[▽] James Marquez, Hu Long, S. Matt Gilbert, Marcus Worsley, and Alex Zettl*

Cite This: *ACS Appl. Nano Mater.* 2021, 4, 3500−3507 Read Online

ACCESS | Metrics & More | Article Recommendations

ABSTRACT: We describe a robust and scalable method to produce crinkled hexagonal boron nitride (h-BN) nanofoam from graphite in a single-step, leapfrog-like process. The conversion is based on carbothermic reduction and simultaneous nitrogenization of boron oxide and graphite. High-resolution transmission electron microscopy and electron diffraction demonstrate that the final converted h-BN nanofoam is crystalline at the atomic scale but has substantial crinkling of the h-BN sheets at the nanoscale. It also supports a dense network of nanometer-sized pores throughout. The operative conversion mechanism from flat carbon precursors to crinkled boron nitride sheets is proposed. Crinkled h-BN nanofoam shows a surface area over 60 times larger, as compared to the graphitic scaffold, leading to improved oil absorption capabilities (up to 325 wt %).

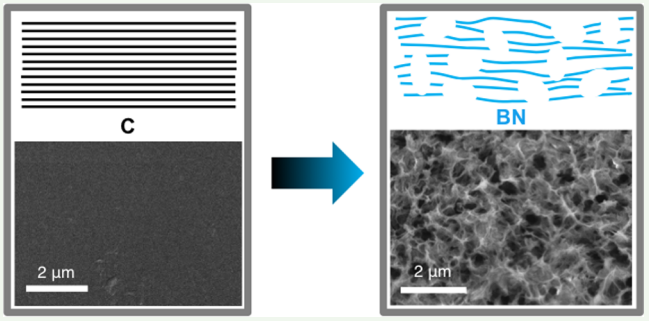

KEYWORDS: *hexagonal boron nitride, graphite, nanofoam, crinkled BN nanosheets, carbothermic conversion*

INTRODUCTION

Three-dimensional, porous, macroscopic structures such as aerogels and rigid foams have shown great efficacy in a wide range of applications, from energy storage,[1] to gas sensing,[2,3] to thermal management for heat transfer,[4] and to the absorption of oleophilic species in aqueous systems.[5,6] Interestingly, such open structures can be derived not only from conventional three-dimensional materials such as oxides but also from low-dimensional building blocks, such as graphene, hexagonal boron nitride (h-BN), and transition-metal dichalcogenides.[7−9] The properties of the final structures are controlled not only by the inherent material properties of the building blocks but also by the connectivity chemistry and geometry, which ultimately affect the porosity, surface area, and chemical and thermal stability of the aerogels and foams.[2,5,9,10]

An impressive array of aerogels and foams are carbon-based, the synthesis of which exploits well-known carbon chemistry. Examples include graphitic aerogels and activated carbon foams.[7,10] Many of the synthetic approaches are of the "bottom-up" variety, where either small particles or molecules are functionalized and covalently bound together to form the macroscopic structure.[11] For carbon, there is a veritable treasure trove of molecular precursors and synthetic routes to choose from, allowing for wide-ranging creativity in aerogel and nanofoam design.[2,12−16]

An exciting complement to carbon, h-BN, has also been explored in various macrostructures. Indeed, h-BN aerogels and foams have been produced and they indicate impressive efficacy in chemical sensing, gas adsorption, atomic sequestering, and membrane composites.[4,17−19] Unfortunately, the diverse synthetic routes endemic to carbon do not typically carry over to h-BN systems, due to a reduced number of boron- and nitrogen-derived starting materials, and generally higher reaction activation barriers. Nevertheless, important contributions have been made in the functionalization of boron nitride (BN) nanosheets to allow for covalent cross-linking of the sheets to generate networks, as well as the direct synthesis of BN structures (such as foams) from molecular precursors of boron- and nitrogen-containing compounds.[4,17,19]

In order to bypass the need for molecular precursors, "top-down" synthetic methods, or conversions, can be pursued. Due to the structural similarity between graphene and h-BN, h-BN macrostructures, such as nanotubes, aerogels, activated powder, and foams, can be synthesized from a sacrificial carbon structure, provided that the carbon is preformed precisely into the desired final structural geometry.[5,9,19−21]

Received: January 1, 2021
Accepted: March 18, 2021
Published: March 30, 2021

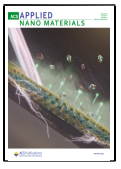

https://doi.org/10.1021/acsanm.1c00003
ACS Appl. Nano Mater. 2021, 4, 3500−3507

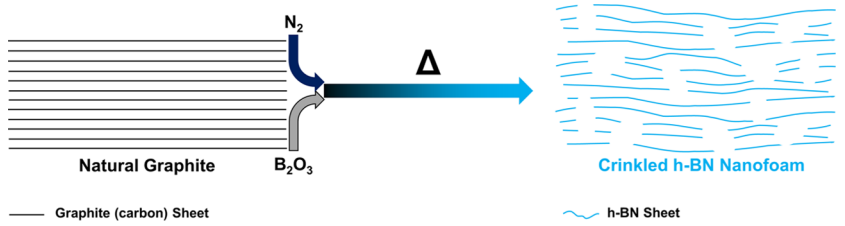

Figure 1. Schematic of the single-step "leapfrog" synthesis of crinkled h-BN nanofoam from natural graphite.

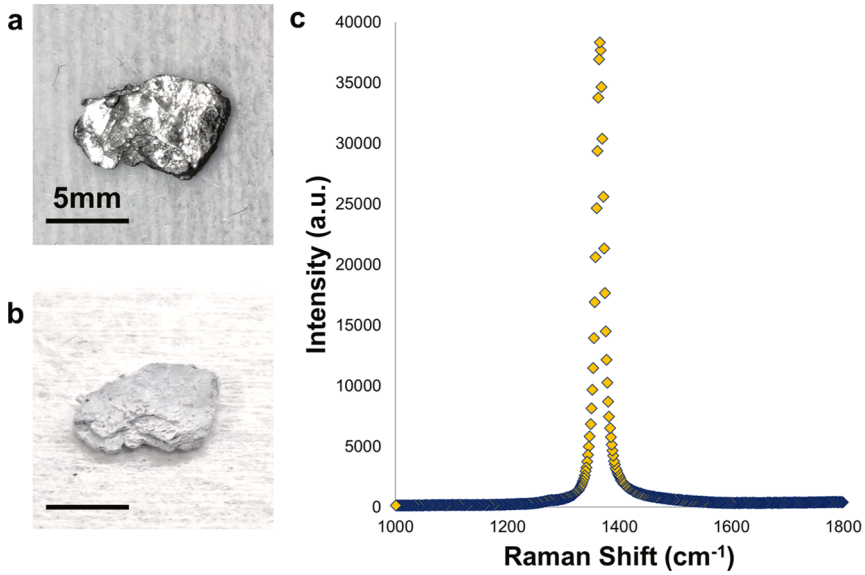

Figure 2. Conversion of graphite fragment to crinkled h-BN nanofoam. Prior to the conversion reaction (a), the graphite fragment is shiny black. After conversion (b), the fragment retains its overall geometry but changes color to bright white. Scale bars in (a,b) measure 5 mm. (c) Raman spectrum of the converted h-BN fragment, with a peak at 1367 cm^{-1} corresponding to the E_{2g} in-plane vibrational mode of sp^2-bonded BN.

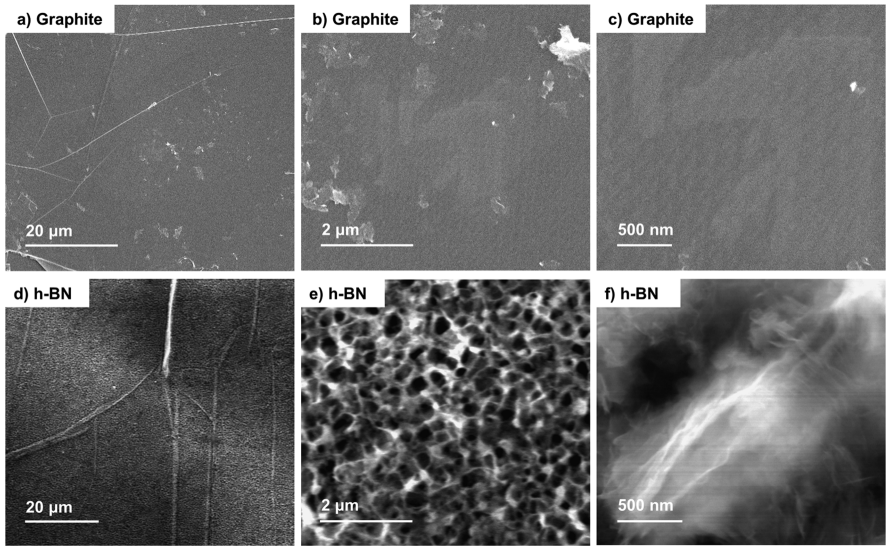

Figure 3. SEM images of (a−c) graphite fragment and (d−f) converted h-BN. The macroscopic morphology of the graphite fragment (a) is maintained in the converted BN (d), where the surface overall is very flat in nature, and even large macroscopic edges and wrinkles can be observed in both (a,d). The flat, pristine nature of the layers in the unconverted graphite fragment is maintained at high magnification, as shown in (b,c). (e) Higher magnification image highlighting the spongy, foam-like nature of the converted h-BN. (f) High magnification SEM image of the h-BN where the crinkled nature of the h-BN sheets is readily visible.

Following such a delicate "two step" process can be extremely time- and energy-intensive.

In this report, we present a facile approach to "leapfrog" the two-step conversion process. We present a one-step method of generating crinkled h-BN nanofoam quickly and directly from raw graphite, as highlighted in Figure 1. The single-step synthetic approach utilizes the simultaneous carbothermic reduction and nitrogenization of boron oxide powder, with

https://doi.org/10.1021/acsanm.1c00003
ACS Appl. Nano Mater. 2021, 4, 3500−3507

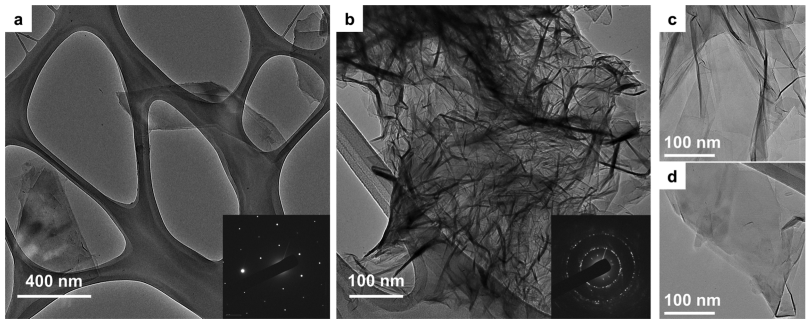

Figure 4. (a) HR-TEM image of flat and well-stacked graphene sheets. (Inset) Corresponding SA-ED pattern showing a unique set of six-spots, indicating single-crystal graphene sheets. (b) HR-TEM image of crinkled, few-layered h-BN from the converted nanofoam. (Inset) Corresponding SA-ED pattern showing several sets of six-spot patterns, indicating rotational and translational stacking in the layered, crinkled sheets. Additional HR-TEM images highlighting (c) mildly crinkled h-BN sheets and (d) almost perfectly flat h-BN sheets from the same h-BN nanofoam sample.

graphite fragments acting as both a source of carbon for the reduction process and instantly a rough template for the growth of the final h-BN product. The h-BN nanofoam is highly crystalline on the atomic scale and is composed of h-BN sheets with varying degrees of crinkling on the nanoscale. An overall porous, foam-like macrostructure is produced that is very amenable to oil absorption due to the drastic increase in surface area from the original starting graphitic material.

RESULTS AND DISCUSSION

The "leapfrog" conversion of graphite to crinkled, h-BN nanofoam, achieved through high-temperature carbothermic reduction of graphite and boron oxide, is highlighted in Figure 2. As illustrated, the overall dimensions of the graphite fragment are retained following conversion (Figure 2a,b), but there is a striking change in color upon conversion, from black to white, indicative of a dramatic chemical modification and a change in the electronic band structure of the material. Figure 2c shows, for the converted material, the unique Raman signature of the E_{2g} in-plane vibrational mode of sp^2-bonded h-BN, at 1367 cm^{-1}.[8] No other peak is observed, consistent with a complete chemical conversion from graphite to h-BN. The resulting h-BN nanofoam expands because of the difference in the morphology from the starting graphite material, and it is qualitatively much more compressible than the parent graphite. Small deformations appear to be reversible, but large deformations lead to fracturing of the material, unlike for some graphene-based aerogel materials.[22]

The structure of the converted material is examined using secondary electron microscopy (SEM), where the conversion from flat graphite to crinkled h-BN nanofoam can be readily seen. The scale of the folds, crinkles, and curvature of the sheets is examined in more detail, as shown in Figure 3, where SEM images are compared at different magnifications of the starting graphite fragment to those obtained (at identical magnification) for the converted crinkled h-BN nanofoam.

Figure 3a shows the macroscopic view of a graphite flake, where several wrinkles in the sheet are readily observed (they appear as bright lines). These wrinkles are anywhere from 20 to 100 μm in length and separated by tens of microns. At higher magnification, as seen in Figure 3b,c, at the 2 μm and 500 nm size scale, regions between the global wrinkles are easily found, and no additional interesting features are observed in graphite. Figure 3d shows a macroscopic view of the h-BN nanofoam, where wrinkles (again appearing as bright lines) ranging from 20 to 100 μm in length are observed, similar to the graphite precursor. However, in sharp contrast, Figure 3e,f shows that for the converted h-BN material, the apparently flat morphology at the 20 μm scale is actually composed of a highly porous nanofoam structure at the 2 μm and 500 nm size scale. At the higher magnification, we see that the character of the h-BN sheets is actually of a porous, foam-like nature, with characteristic pores and linkers on the order of 500 nm to 1 μm in length. This new porous morphology covers the entire surface of the h-BN nanofoam. We refer to the overall surface of the h-BN as crinkled to delineate between a specific isolated large-scale wrinkle in the material and the overall surface morphology of the nanofoam. The pores vary somewhat in size, but are typically 500 nm across, as shown in Figure 3f, with high areas of curvature surrounding the pores, leading to the crinkled effect.

In contrast to the more conventional carbon-to-h-BN templating conversion process, the simplified one-step conversion method presented here apparently completely leapfrogs the need for first preparing a porous carbon intermediary. In most previous carbon-to-boron-nitride conversions, such as C-to-BN nanotubes,[20] C-to-BN aerogels,[5,9] and C-to-BN activated powder,[21] both the macroscopic and nanoscopic structures of the carbon precursors are maintained in the corresponding BN products. Hence, the carbon-based starting material must first be configured into the desired "end form". Here, the converted h-BN has a similar macroscopic structure as the starting graphite (i.e., layered "sheets" of material) but displays drastically different nanoscopic structures (i.e., crinkled nanofoam). In discussion below, we examine the likelihood that a nanoporous carbon intermediate structure is involved but is "automatically" locally formed within the graphite and then quickly templated and converted to crinkled nanoporous h-BN foam.

In addition to the change in the structure from conversion of graphite to h-BN nanofoam, we are also interested in how the properties of the resulting crinkled nanofoam differ from the graphitic precursor. Native graphite has incredibly low surface areas of roughly 0.6 m^2/g and is moderately hydrophilic in nature.[23,24] We find that the crinkled nature of the h-BN nanofoam presented in this study exhibits surface areas of 41.2 $\pm$ 0.8 m^2/g, an increase in surface area over 60 times from the graphitic precursor. The surface area of this single-step converted, crinkled h-BN nanofoam is well within the desired range of other h-BN foams (30 to 130 m^2/g) and substantially higher than carbon-based nanofoams from other commonly used carbon precursors (0.16 to 3.3 m^2/g), all without requiring an involved, multistep synthesis process.[17,25,26] Along

https://doi.org/10.1021/acsanm.1c00003
ACS Appl. Nano Mater. 2021, 4, 3500−3507

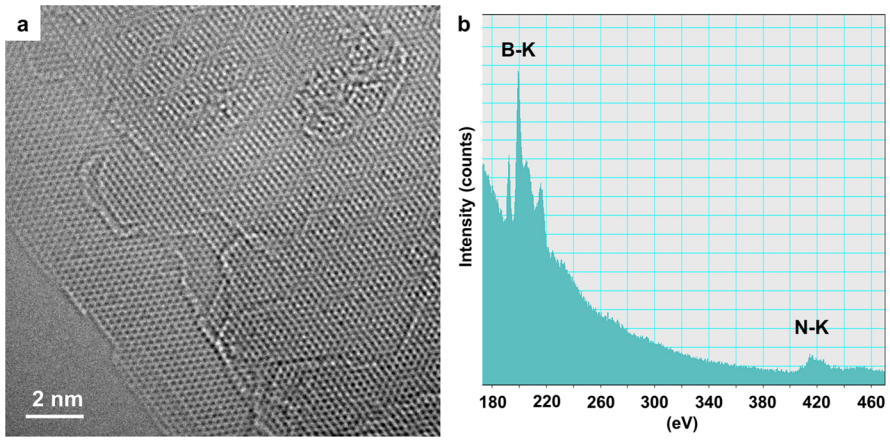

Figure 5. (a) AC atomic-resolution TEM image of converted few-layer h-BN taken from the crinkled nanofoam, showing a single-layered edge and triangular defects, as well as a Moiré pattern in the few-layered region. (b) Elemental composition confirmed by corresponding EELS spectrum displaying K-edges of boron (B) and nitrogen (N). The extracted atomic ratio is 1B/1N.

with a drastic increase in surface area, the crinkled h-BN nanofoams are more hydrophobic than graphite, allowing for improved oil absorption capabilities. We find oil absorption rates up to 325 wt %, twice as efficient as other commonly used activated carbon alternatives.[5,6]

The crystallinity and chemical makeup of the crinkled h-BN sheets forming the nanofoam are examined further using transmission electron microscopy (TEM). Figure 4 shows typical TEM images of graphite sheets before conversion and h-BN sheets after conversion, using the one-step conversion process. Figure 4a shows a TEM image of the starting graphite sample (mechanically exfoliated to facilitate TEM imaging); it displays the well-known flat graphene structure. The corresponding selected area electron diffraction (SA-ED, Figure 4a inset) shows that the few-layer graphene sheets are single crystal, evidenced by a unique set of six bright spots representing the graphene hexagonal lattice. The atomic morphology of the converted h-BN sheets is shown in Figure 4b–d. Here, although a sheet-like structure is clearly still evident, the sheets are no longer flat but possess various degrees of crinkling. The SA-ED inset in Figure 4b correspondingly exhibits many sets of spots with six-fold symmetry, indicating atomic crystallinity but with changing of stacking sequences and rotation of the sheets due to the severity of the crinkling.

At the size scale, as shown in Figure 4, sheets from the h-BN nanofoam may exhibit different degrees of curvature in their crinkling. Some regions have very high curvature (Figure 4b), medium curvature (Figure 4c), and almost no curvature (Figure 4d). However, the overall morphology of the crinkled h-BN nanofoam is uniform in distribution of these various degrees of crinkling. A crinkled piece of paper would exhibit similar differences in the morphology at small size scales, where the crinkling of the paper is globally uniformly distributed across the surface, but regions of almost perfectly flat surface will be found between regions of extremely high curvature.

We then employ aberration-corrected (AC)-TEM and electron energy loss spectroscopy (EELS) to probe in greater detail the crystallinity and chemical purity of the converted h-BN material. The results are shown in Figure 5. AC-TEM imaging (Figure 5a) clearly shows the hexagonal lattice in the sheets of the converted h-BN nanofoam. At the edge of the sheets, where there are approximately three layers of hexagonal BN, the layers stack perfectly in the conventional AA′ order, evidenced by the well-aligned hexagons of B and N atoms, with N-terminated zig-zag edges.[27] We also observe the signature triangular electron-induced defects commonly seen in h-BN during electron microscopy imaging.[28] Interestingly, moving toward the center of the sample (toward the top right corner of the AC-TEM image), several Moiré patterns are observable, indicative of the changing of stacking sequences, either by a translational or rotational shifting of the top sheets with respect to the bottom ones.[27,29] The change in the stacking sequence is a result of the crinkling observed in the h-BN sheets. The corresponding EELS spectrum (Figure 5b) shows that the converted h-BN sheets contain only B and N atoms, with an atomic ratio of 1B/1N. There is no C edge found in the spectrum, confirming the chemical purity of the sample. These studies confirm the complete conversion from the crystalline, flat graphite fragment to atomically crystalline, crinkled h-BN nanofoam.

We now examine the formation mechanism of the crinkled h-BN nanofoam. As mentioned previously, in conventional carbon templating, the bulk and nanoscale structural morphology of the parent carbon-based material is maintained in the final BN product. This follows naturally from the isoelectronic hexagonal structure of graphene and h-BN and the near-identical lattice parameters. An interesting question is what reaction path is followed in the present one-step conversion process, where the morphology is clearly dramatically altered, at least at the nanoscale.

In general, a carbothermic reduction starts with the reduction of an oxide, in this case boron oxide, by carbon atoms from a carbon source, in this case graphite. During the reduction process, nitrogenization of the products can be simultaneously incorporated to produce a final BN product. While the graphite flakes and boron oxide are solid reagents, the B_2O_3 vaporizes and becomes a gaseous reagent alongside the N_2 during heating. The carbothermic reduction and nitrogenization occurs at the atomic sites of the carbon source, which generally means that the carbon source is gradually replaced by BN. In the case of this experiment, the carbon source is the hexagonal carbon lattice of graphite, which is gradually replaced with an h-BN lattice,[30]

https://doi.org/10.1021/acsanm.1c00003
ACS Appl. Nano Mater. 2021, 4, 3500−3507

$$\frac{3}{2}C(s) + B_2O_3(g) + N_2(g) \xrightarrow{\Delta} 2BN(s) + \frac{3}{2}CO_2(g) \quad (1)$$

The reaction described in eq 1 likely preferentially starts at defect sites in the carbon materials, such as surface functional groups, wrinkles, grain boundaries, vacancies, and edge atoms, where there is weaker bonding compared to the flat surface of a pristine sheet of sp^2-bonded carbon atoms.[20,31] For many previously studied carbon materials, such as carbon nanotubes or graphene aerogels, the material comprises micron- or nano-sized features with a large active surface area, containing many pathways for the boron- and nitrogen-containing gaseous species to approach the graphitic structure and react.[9] In contrast, for thick high-quality graphite fragments many hundreds of microns in size, the only accessible sites for the incoming gaseous reactant are the undersaturated bonds on the carbon atoms at edges or the relatively rare wrinkles in the sheets of the graphite layers. We hypothesize that, as a result, the conversion reaction preferentially starts from the edges of the graphite layers, and to some extent the top and bottom surfaces of the layers as well, and proceeds inward from there.[30]

The crinkling of the layers occurs throughout the conversion process as the final product (h-BN) and any intermediate products have different thermal expansion coefficients and lattice mismatches compared to the supporting graphite layers.[32−34] As mentioned, the graphite flakes comprise many layers of micron-sized graphene sheets densely stacked together, resulting in stepwise conversion from outside-in. As a result, at elevated reacting temperatures, the expansion mismatch, between the lattice of graphene versus h-BN and any intermediates in a densely packed and micron-sized system, would induce buckling and crinkling of the sheets. The pores of the h-BN nanofoam are created as the sheets crinkle during the conversion process. Because the pores are formed by the sheets crinkling, which is ultimately controlled by the difference in thermal expansion of the graphene layers, h-BN layers, and any intermediates, the pore size is relatively fixed and provides consistency between the samples synthesized and analyzed.

In order to test this hypothesis and to better understand how the conversion process migrates through the graphite layers, a related conversion experiment is performed on a relatively large graphite fragment ~1 cm in size. The larger graphite fragment is intentionally only partially converted to h-BN by limiting the boron oxide present in the system and reaction time. The partially converted sample is then cleaved to identify different regions with different degrees of conversion, with regions near the center of the sample having the lowest degree of conversion.

We note that large samples such as this can be completely converted through the entirety of the flake, but the diffusion of the gaseous reagents is the time-limiting factor. If standard diffusion of the gaseous reagents is assumed, then the time the conversion takes scales (assuming standard diffusion theory) as the square of the size of the sample. So, as an example, if the 5 mm sample of Figure 2 is converted in 1 h, a 10 mm sample (such as the one shown in Figure 6) would take 4 h for complete conversion. If this leapfrog conversion technique was applied to a 50 mm sample, the overall reaction time might take up to 100 h. We see no evidence that long processing times degrade already converted material (say at the outer surface of the specimen, where conversion first occurs). On the other hand, the h-BN nanofoam expands throughout the conversion process, further aiding the diffusion of the gaseous reagents to penetrate the sample, thus speeding up the conversion process. In our current experimental setup, reaction times can be long, but the limited availability of boron oxide would prevent full conversion of very large samples. Of course,

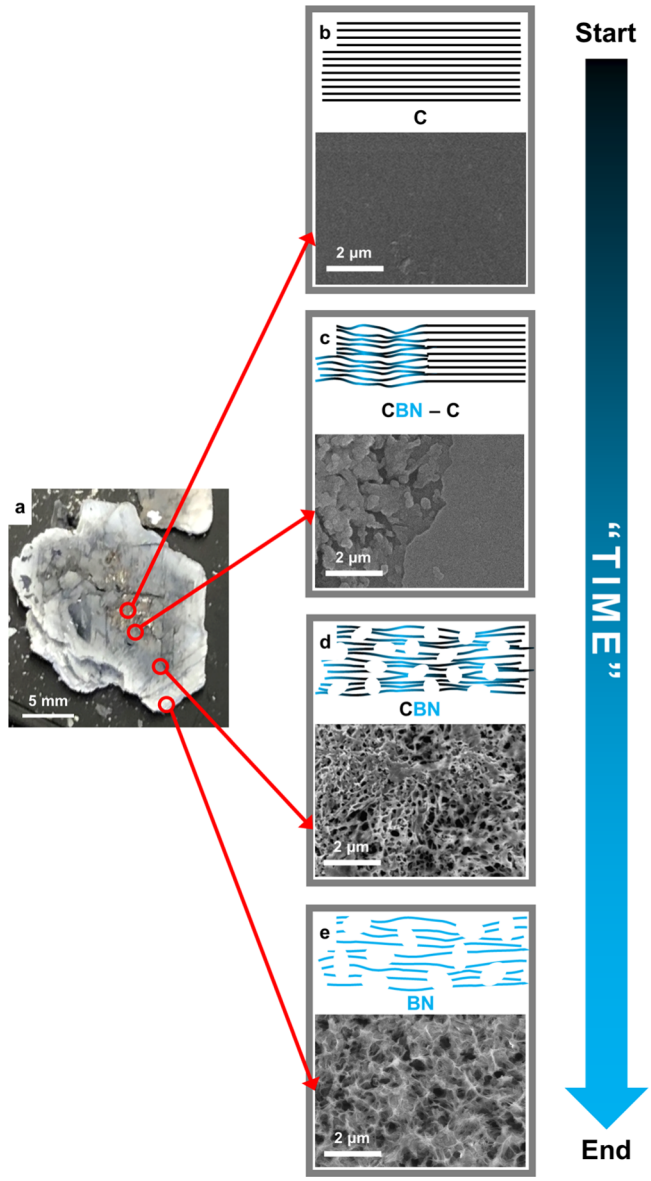

Figure 6. Bulk graphite to crinkled h-BN nanofoam reaction progression. The conversion of a single large graphite fragment is interrupted midstream such that only the outer surface of the fragment is fully converted, while further in the sample is partially converted, and, at the very core, still pristine and unconverted. Materials taken from different regions thus present a "time" series of the conversion reaction. (a) Optical photograph of the bulk fragment. (b−e) SEM images for materials taken from the core (b), mid-regions (c,d), and outer edge (e). Schematics above each SEM image represent the nanostructure and chemical composition, ranging from flat planes of pure carbon graphite in (b) to fully converted, high-porosity crinkled sheets of h-BN nanofoam in (e); they suggest a likely conversion pathway (see the main text). Black color in the schematics represents carbon, while blue color represents BN. The letters C, CBN, and BN represent pure carbon, a carbon−boron−nitride mixture, and pure boron nitride, respectively.

https://doi.org/10.1021/acsanm.1c00003
ACS Appl. Nano Mater. 2021, 4, 3500−3507

the experimental setup could be reconfigured to a flow-type system, where boron oxide could be heated separately from the graphite flake, and subsequently flowed in, which would present itself as a more ideal system for large-scale conversion.

Figure 6 presents results from the conversion progression experiment. Figure 6a is an optical microscope image of the large, partially converted graphite fragment. After cleaving, the fragment retains its white edges, suggestive of complete conversion to h-BN, while the center is black, suggestive of unconverted graphite. Off-center regions are gray, suggestive of a carbon−boron−nitride mixture. Figure 6b−e shows SEM images for material taken from different regions of the sample, Figure 6b shows SEM images for material taken from the center region, and Figure 6e shows SEM images from the edge region. Figure 6c,d shows SEM images for material taken from intermediate regions. The upper halves of Figure 6b−e are illustrative schematics of the nanoscale structure of the corresponding regions, with black representing carbon-based material and blue representing BN-based material. The letters C, CBN, and BN stand for carbon, carbon−boron−nitride mixture, and pure BN, respectively. In a sense, the progression from Figure 6b−e represents a time progression of the reaction from "start" to "end", hence our addition of a "time" arrow in the figure, whose color gradually changes from black to blue.

The conversion process produces intermediate CBN material, with different atomic ratios throughout the sample, depending on progression of the reaction. The largely unconverted graphite material of Figure 6b is smooth and featureless with well-ordered carbon-based parallel planes. The beginnings of h-BN conversion are seen in the intermediate structure of Figure 6c, where a boundary exists between the graphitic carbon and crinkled BN. Macroscopically, the material now appears gray. Figure 6d represents further progression into the conversion reaction. The material continues to appear gray, but the conversion of the sheets to crinkled h-BN has progressed, and numerous nanoscale pores have appeared. The material resembles a foam. For the fully converted material, Figure 6e, the product consists of crinkled, pure h-BN nanofoam, strikingly white. These observations reinforce an outside-in conversion mechanism and pathway, where the graphite is converted at an extremely local level to crinkled h-BN nanofoam.

CONCLUSIONS

In this study, we introduce a "leapfrog" conversion method as a single-step, cost-effective, and scalable method of preparing crinkled h-BN nanofoam for oil absorption via the carbothermic reduction and nitrogenization of boron oxide and graphite. The crinkled h-BN nanofoam maintains some aspects of the macroscopic properties of the precursor graphite, namely, a sheet-like surface of large domains with wrinkles and edges. However, critically, the surface exhibits a dense network of pores on the nanometer size scale, reflecting pure h-BN nanofoam, and results in a significantly higher surface area for the nanofoam, as compared to the graphitic starting species. The crystallinity and chemical makeup of the h-BN nanofoam are confirmed by AC-TEM and EELS. A conversion pathway is presented for flat graphite sheets to crinkled-sheet h-BN nanofoam. The resultant h-BN nanofoams find significant improvement in the absorption of oil, as compared to other activated carbon species, and the increased surface area could find use in other applications, such as chemical sensing, gas storage/capture, and membrane composites.

METHODS

Material Synthesis. The high-temperature carbothermic-reduction synthesis method for crinkled h-BN nanofoam uses components of a synthesis method for BN aerogels, as reported elsewhere.[5,9] Briefly, a pure and un-restructured graphite precursor is placed together with boron oxide in a custom machined graphite crucible and heated to between 1650 and 1850 °C in an induction furnace under a pure nitrogen gas flow.

Several different graphite precursors are examined with different domain sizes and crystallinity, namely, highly ordered pyrolytic graphite, Kish graphite, few-micron-sized graphite flake powder, and centimeter-sized graphite fragments. Typically, up to 0.5 g of graphite is loaded in the graphite crucible, together with excess boron oxide, usually 5−10 g depending on the amount of graphite material being converted. Nitrogen gas is flowed through the system at 1500 sccm, and total reaction time is 60 min to ensure a complete conversion. The converted h-BN nanofoam obtained from the different graphite precursors all show comparable results, so for simplicity and consistency, all data presented in this report are obtained from the conversion of naturally occurring graphite fragments [Alfa Aesar, Graphite flake, 325 mesh, 99.8% (metal basis)].

Material Characterization. Raman spectroscopy is performed using a Renishaw inVia spectrometer with 514 nm laser excitation. Structural information and atomic imaging are obtained using scanning electron microscopy (FEI Sirion XL30) and TEM (JEOL JEM 2010 and AC TEAM 0.5, both operated at 80 kV), respectively. Nitrogen porosimetry was determined by the Brunauer−Emmett−Teller (BET) method using an ASAP 2020 surface area analyzer (Micromeritics Instrument Corporation).

AUTHOR INFORMATION

Corresponding Author

Alex Zettl − *Department of Physics and Kavli Energy NanoSciences Institute, University of California at Berkeley, Berkeley, California 94720, United States; Materials Science Division, Lawrence Berkeley National Laboratory, Berkeley, California 94720, United States*; Email: azettl@berkeley.edu

Authors

Thang Pham − *Department of Physics and Department of Materials Science and Engineering, University of California at Berkeley, Berkeley, California 94720, United States;* orcid.org/0000-0001-5940-6206

Scott Stonemeyer − *Department of Physics, Department of Chemistry, and Kavli Energy NanoSciences Institute, University of California at Berkeley, Berkeley, California 94720, United States; Materials Science Division, Lawrence Berkeley National Laboratory, Berkeley, California 94720, United States;* orcid.org/0000-0002-8135-5625

James Marquez − *Department of Physics, University of California at Berkeley, Berkeley, California 94720, United States*

Hu Long − *Department of Physics, University of California at Berkeley, Berkeley, California 94720, United States;* orcid.org/0000-0002-7983-0749

S. Matt Gilbert − *Department of Physics, University of California at Berkeley, Berkeley, California 94720, United States*

Marcus Worsley − *Physical and Life Sciences Directorate, Lawrence Livermore National Laboratory, Livermore, California 94550, United States*

https://doi.org/10.1021/acsanm.1c00003
ACS Appl. Nano Mater. 2021, 4, 3500−3507

Complete contact information is available at:
https://pubs.acs.org/10.1021/acsanm.1c00003

Author Contributions

[▽]T.P. and S.S. contributed equally.

Notes

The authors declare no competing financial interest.

■ ACKNOWLEDGMENTS

This research was supported by the Director, Office of Science, Office of Basic Energy Sciences, Materials Sciences and Engineering Division, of the US Department of Energy under contract no. DEAC02-05-CH11231, primarily within the sp^2-Bonded Materials Program (KC-2207) which provided for conversion of the crinkled h-BN and in part by the van der Waals Heterostructures program (KCWF16) which provided for Raman spectroscopy analysis. This work was additionally supported by the National Science Foundation under grant # DMR-1807233 which provided for conventional TEM imaging. High-resolution TEM imaging and spectroscopy at the Molecular Foundry were supported by the Office of Science, Office of Basic Energy Sciences, of the US Department of Energy under contract no. DE-AC02-05CH11231. Surface area and BET measurements were performed under the auspices of the U.S. Department of Energy by Lawrence Livermore National Laboratory under contract DE-AC52-07NA27344. S.M.G. acknowledges support from a Kavli Energy Nano Sciences Institute Fellowship and an NSF Graduate Fellowship. The authors thank Dr. Kyunghoon Lee for assistance with material characterization.

■ REFERENCES

(1) Zhu, C.; Liu, T.; Qian, F.; Han, T. Y.-J.; Duoss, E. B.; Kuntz, J. D.; Spadaccini, C. M.; Worsley, M. A.; Li, Y. Supercapacitors Based on Three-Dimensional Hierarchical Graphene Aerogels with Periodic Macropores. *Nano Lett.* **2016**, *16*, 3448−3456.
(2) Turner, S.; Yan, W.; Long, H.; Nelson, A. J.; Baker, A.; Lee, J. R. I.; Carraro, C.; Worsley, M. A.; Maboudian, R.; Zettl, A. Boron Doping and Defect Engineering of Graphene Aerogels for Ultrasensitive NO_2 Detection. *J. Phys. Chem. C* **2018**, *122*, 20358−20365.
(3) Harley-Trochimczyk, A.; Pham, T.; Chang, J.; Chen, E.; Worsley, M. A.; Zettl, A.; Mickelson, W.; Maboudian, R. Platinum Nanoparticle Loading of Boron Nitride Aerogel and Its Use as a Novel Material for Low-Power Catalytic Gas Sensing. *Adv. Funct. Mater.* **2016**, *26*, 433−439.
(4) Ashton, T. S.; Moore, A. L. Foam-like Hierarchical Hexagonal Boron Nitride as a Non-Traditional Thermal Conductivity Enhancer for Polymer-Based Composite Materials. *Int. J. Heat Mass Transfer* **2017**, *115*, 273−281.
(5) Pham, T.; Goldstein, A. P.; Lewicki, J. P.; Kucheyev, S. O.; Wang, C.; Russell, T. P.; Worsley, M. A.; Woo, L.; Mickelson, W.; Zettl, A. Nanoscale Structure and Superhydrophobicity of Sp^2-Bonded Boron Nitride Aerogels. *Nanoscale* **2015**, *7*, 10449−10458.
(6) Zhao, J.; Ren, W.; Cheng, H.-M. Graphene Sponge for Efficient and Repeatable Adsorption and Desorption of Water Contaminations. *J. Mater. Chem.* **2012**, *22*, 20197−20202.
(7) Inagaki, M.; Qiu, J.; Guo, Q. Carbon Foam: Preparation and Application. *Carbon* **2015**, *87*, 128−152.
(8) Worsley, M. A.; Shin, S. J.; Merrill, M. D.; Lenhardt, J.; Nelson, A. J.; Woo, L. Y.; Gash, A. E.; Baumann, T. F.; Orme, C. A. Ultralow Density, Monolithic WS_2, MoS_2, and MoS_2/Graphene Aerogels. *ACS Nano* **2015**, *9*, 4698−4705.
(9) Rousseas, M.; Goldstein, A. P.; Mickelson, W.; Worsley, M. A.; Woo, L.; Zettl, A. Synthesis of Highly Crystalline sp^2-Bonded Boron Nitride Aerogels. *ACS Nano* **2013**, *7*, 8540−8546.
(10) Worsley, M. A.; Pauzauskie, P. J.; Olson, T. Y.; Biener, J.; Satcher, J. H.; Baumann, T. F. Synthesis of Graphene Aerogel with High Electrical Conductivity. *J. Am. Chem. Soc.* **2010**, *132*, 14067−14069.
(11) Gorgolis, G.; Galiotis, C. Graphene Aerogels: A Review. *2D Mater.* **2017**, *4*, 032001.
(12) Qian, Y.; Ismail, I. M.; Stein, A. Ultralight, High-Surface-Area, Multifunctional Graphene-Based Aerogels from Self-Assembly of Graphene Oxide and Resol. *Carbon* **2014**, *68*, 221−231.
(13) Sha, J.; Li, Y.; Villegas Salvatierra, R.; Wang, T.; Dong, P.; Ji, Y.; Lee, S.-K.; Zhang, C.; Zhang, J.; Smith, R. H.; Ajayan, P. M.; Lou, J.; Zhao, N.; Tour, J. M. Three-Dimensional Printed Graphene Foams. *ACS Nano* **2017**, *11*, 6860−6867.
(14) Inagaki, M.; Toyoda, M.; Soneda, Y.; Morishita, T. Nitrogen-Doped Carbon Materials. *Carbon* **2018**, *132*, 104−140.
(15) Tian, W.; Zhang, H.; Duan, X.; Sun, H.; Shao, G.; Wang, S. Porous Carbons: Structure-Oriented Design and Versatile Applications. *Adv. Funct. Mater.* **2020**, *30*, 1909265.
(16) Huang, H.; Shi, H.; Das, P.; Qin, J.; Li, Y.; Wang, X.; Su, F.; Wen, P.; Li, S.; Lu, P.; Liu, F.; Li, Y.; Zhang, Y.; Wang, Y.; Wu, Z. S.; Cheng, H. M. The Chemistry and Promising Applications of Graphene and Porous Graphene Materials. *Adv. Funct. Mater.* **2020**, *30*, 1909035.
(17) Owuor, P. S.; Park, O.-K.; Woellner, C. F.; Jalilov, A. S.; Susarla, S.; Joyner, J.; Ozden, S.; Duy, L.; Villegas Salvatierra, R.; Vajtai, R.; Tour, J. M.; Lou, J.; Galvão, D. S.; Tiwary, C. S.; Ajayan, P. M. Lightweight Hexagonal Boron Nitride Foam for CO_2 Absorption. *ACS Nano* **2017**, *11*, 8944−8952.
(18) Angizi, S.; Khalaj, M.; Alem, S. A. A.; Pakdel, A.; Willander, M.; Hatamie, A.; Simchi, A. Review—Towards the Two-Dimensional Hexagonal Boron Nitride (2D h-BN) Electrochemical Sensing Platforms. *J. Electrochem. Soc.* **2020**, *167*, 126513.
(19) Li, S.; Liu, F.; Su, Y.; Shao, N.; Yu, D.; Liu, Y.; Liu, W.; Zhang, Z. Luffa Sponge-Derived Hierarchical Meso/Macroporous Boron Nitride Fibers as Superior Sorbents for Heavy Metal Sequestration. *J. Hazard. Mater.* **2019**, *378*, 120669.
(20) Han, W.; Bando, Y.; Kurashima, K.; Sato, T. Synthesis of Boron Nitride Nanotubes from Carbon Nanotubes by a Substitution Reaction. *Appl. Phys. Lett.* **1998**, *73*, 3085−3087.
(21) Han, W.-Q.; Brutchey, R.; Tilley, T. D.; Zettl, A. Activated Boron Nitride Derived from Activated Carbon. *Nano Lett.* **2004**, *4*, 173−176.
(22) Hu, H.; Zhao, Z.; Wan, W.; Gogotsi, Y.; Qiu, J. Ultralight and Highly Compressible Graphene Aerogels. *Adv. Mater.* **2013**, *25*, 2219−2223.
(23) Kozbial, A.; Zhou, F.; Li, Z.; Liu, H.; Li, L. Are Graphitic Surfaces Hydrophobic? *Acc. Chem. Res.* **2016**, *49*, 2765−2773.
(24) Shornikova, O. N.; Kogan, E. V.; Sorokina, N. E.; Avdeev, V. V. The Specific Surface Area and Porous Structure of Graphite Materials. *Russ. J. Phys. Chem. A* **2009**, *83*, 1022−1025.
(25) Jiang, H.; Ma, L.; Yang, Q.; Tang, Z.; Song, X.; Zeng, H.; Zhi, C. Three-Dimensional Porous Boron Nitride Foam for Effective CO_2 Adsorption. *Solid State Commun.* **2019**, *294*, 1−5.
(26) Chen, C.; Kennel, E. B.; Stiller, A. H.; Stansberry, P. G.; Zondlo, J. W. Carbon Foam Derived from Various Precursors. *Carbon* **2006**, *44*, 1535−1543.
(27) Alem, N.; Erni, R.; Kisielowski, C.; Rossell, M. D.; Gannett, W.; Zettl, A. Atomically Thin Hexagonal Boron Nitride Probed by Ultrahigh-Resolution Transmission Electron Microscopy. *Phys. Rev. B: Condens. Matter Mater. Phys.* **2009**, *80*, 1−7.
(28) Pham, T.; Gibb, A. L.; Li, Z.; Gilbert, S. M.; Song, C.; Louie, S. G.; Zettl, A. Formation and Dynamics of Electron-Irradiation-Induced Defects in Hexagonal Boron Nitride at Elevated Temperatures. *Nano Lett.* **2016**, *16*, 7142−7147.
(29) Kim, K.; Lee, Z.; Malone, B. D.; Chan, K. T.; Alemán, B.; Regan, W.; Gannett, W.; Crommie, M. F.; Cohen, M. L.; Zettl, A. Multiply Folded Graphene. *Phys. Rev. B: Condens. Matter Mater. Phys.* **2011**, *83*, 245433.

(30) Bando, Y.; Golberg, D.; Mitome, M.; Kurashima, K.; Sato, T. C to BN Conversion in Multi-Walled Nanotubes as Revealed by Energy-Filtering Transmission Electron Microscopy. *Chem. Phys. Lett.* **2001**, *346*, 29−34.
(31) Han, W.-Q.; Cumings, J.; Huang, X.; Bradley, K.; Zettl, A. Synthesis of Aligned $B_xC_yN_z$ Nanotubes by a Substitution-Reaction Route. *Chem. Phys. Lett.* **2001**, *346*, 368−372.
(32) Singh, S. K.; Neek-Amal, M.; Costamagna, S.; Peeters, F. M. Thermomechanical Properties of a Single Hexagonal Boron Nitride Sheet. *Phys. Rev. B: Condens. Matter Mater. Phys.* **2013**, *87*, 1−7.
(33) Tsang, D. K. L.; Marsden, B. J.; Fok, S. L.; Hall, G. Graphite Thermal Expansion Relationship for Different Temperature Ranges. *Carbon* **2005**, *43*, 2902−2906.
(34) Thévenot, F. Boron Carbide-A Comprehensive Review. *J. Eur. Ceram. Soc.* **1990**, *6*, 205−225.

https://doi.org/10.1021/acsanm.1c00003
ACS Appl. Nano Mater. 2021, 4, 3500−3507